AAPG Bulletin

The role of mechanically weak layers in controlling fault kinematics and graben configurations: an analogue experimental approach with examples from the Norwegian continental margin

--Manuscript Draft--

Manuscript Number:	
Full Title:	The role of mechanically weak layers in controlling fault kinematics and graben configurations: an analogue experimental approach with examples from the Norwegian continental margin
Article Type:	Article
Keywords:	Analogue experiments; stratified sedimentary sequences; graben geometry; extensional faults style; Norwegian continental margin
Corresponding Author:	Roy Helge Gabrielsen Universitetet i Oslo Oslo, Oslo NORWAY
Corresponding Author Secondary Information:	
Corresponding Author's Institution:	Universitetet i Oslo
Corresponding Author's Secondary Institution:	
First Author:	Roy Helge Gabrielsen
First Author Secondary Information:	
Order of Authors:	Roy Helge Gabrielsen
	Heleen Zalmstra
	Dimitrios Sokoutis
	Ernst Willingshofer
	Jan Inge Faleide
	Hanna Lima Braut
Order of Authors Secondary Information:	
Manuscript Region of Origin:	NORWAY
Abstract:	Faults in extensional basins commonly display geometries that vary with depth, presumably reflecting depth- and lithology-dependent mechanical strength. We address this important relationship by investigating stratified sequences consisting of brittle (sand) and brittle-ductile (sand-silicone polymer). We subject the sand-silicone polymer sequence by multistage extensional deformation through physical analogue experiments. Experiments (series 1) using homogeneous and stratified quartz and feldspar sand produced asymmetric, composite single grabens with diverse fault frequency and fault style for the graben margin faults. For the mechanically stratified experiments with one décollement level (series 2), contrasting graben configurations were produced and that the lowermost sequence was characterized by graben geometries of similar type to that of the series 1 experiments, whereas the upper sequence was strongly influenced by large fault blocks delineated by over-steepened marginal faults sliding above the silicone layer. The experiments with two décollements (series 3) displayed similar, but widening-upward graben geometries, each level being characterized by independent fault systems. The marginal faults of the grabens were soft-linked and in some cases hard-linked, thus contributing to a generally consistent graben geometry at those levels. The results can be used in explaining the contrasting fault patterns and the depth-dependent extension at different levels as seen in several places in the Norwegian

	continental margin and elsewhere.
Suggested Reviewers:	Conrad Childs conrad.childs@ucd.ie Specialist in basin fault analysis
	Martha Withjack drmeow3@rci.rutgers.edu Specialist in basin fault analysis
	Erik Lundin erlun@statoil.com Specialist in basins analysis and petroleum exploration
	Gary Couples Gary.Couples@pet.hw.ac.uk Spesialist in geophysics and fracture tectonics
	John J. Walsh john.walsh@ucd.ie Specialist in basin fault analysis
Opposed Reviewers:	
Additional Information:	
Question	**Response**

The role of mechanically weak layers in controlling fault kinematics and graben configurations: an analogue experimental approach with examples from the Norwegian continental margin.

Update 5.February, 2017

Roy H. Gabrielsen[1)], Heleen Zalmstra[1)], Dimitrios Sokoutis[1,2)], Ernst Willingshofer[2)], Jan Inge Faleide[1)] & Hanna Lima Braut[1,3]

1) Department of Geosciences, University of Oslo, Norway
2) Faculty of Geosciences, Department of Earth Sciences, Utrecht University, Utrecht, The Netherlands
3) Aker BP, Stavanger

Corresponding author: Roy H. Gabrielsen; r.h.gabrielsen@geo.uio.no

Abstract

Faults in extensional basins commonly display geometries that vary with depth, presumably reflecting depth- and lithology-dependent mechanical strength. We address this important relationship by investigating stratified sequences consisting of brittle (sand) and brittle-ductile (sand-silicone polymer). We subject the sand-silicone polymer sequence by multistage extensional deformation through physical analogue experiments.

Experiments (series 1) using homogeneous and stratified quartz and feldspar sand produced asymmetric, composite single grabens with diverse fault frequency and fault style for the graben margin faults.
For the mechanically stratified experiments with one décollement level (series 2), contrasting graben configurations were produced and that the lowermost sequence was characterized by graben geometries of similar type to that of the series 1 experiments, whereas the upper sequence was strongly influenced by large fault blocks delineated by over-steepened marginal faults sliding above the silicone layer.
The experiments with two décollements (series 3) displayed similar, but widening-upward graben geometries, each level being characterized by independent fault systems. The marginal faults of the grabens were soft-linked and in some cases hard-linked, thus contributing to a generally consistent graben geometry at those levels.
The results can be used in explaining the contrasting fault patterns and the depth-dependent extension at different levels as seen in several places in the Norwegian continental margin and elsewhere.

Key words: Analogue experiments, multistage deformation, stratified sedimentary sequences, graben geometry, extensional faults style, Norwegian continental margin.

Introduction

Contrasting fault patterns (fault style and frequency) at different stratigraphic levels in sediment sequences due to lithological contrasts and thus mechanical strength are common in contractional (e.g. Froitzheim & Eberli, 1990, Grelaud et al., 2003, Briggs et al., 2006, Bruton et al., 2010, Chapman & McCarty, 2013, Perrin et al., 2013) as well extensional systems (e.g. Gabrielsen 1984; Harvey & Stewart 1998; Withjack & Callaway 2000; Dooley et al. 2003; Dutton & Trudgill, 2009; Wilson et al. 2013; Jackson & Lewis 2012; Gabrielsen et al 2016). Décollement layers are commonly associated with distinct stratigraphic levels such as evaporite or mudstone (Brun & Choukroune 1989; Koyi & Petersen, 1993, Stewart, 1993, Withjack & Callaway, 2000, Marsh et al., 2010, Jackson & Lewis 2012; Wilson et al., 2013). It is generally assumed that layer-parallel décollements are affiliated with distinct bedding-parallel, sub-horizontal sole faults (Gabrielsen 1984; Gibbs, 1984; Fossen & Gabrielsen, 1995; Wijns et al., 2005; Latta & Anastasio 2007), but intra-formational flow in stratigraphically thick sequences can create conditions where strain is more evenly distributed within the weak unit (Edwards, 1976, Harvey & Stewart 1998; Marsh et al. 2010; Anell et al., 2013; Jackson & Lewis 2012; Gabrielsen et al. 2016). Décollements in extensional fault systems are common in many basins worldwide, like in the Northern Alboran Basin in the Betics (García-Dueñas et al., 1992), the Naxos and Paros islands in Greece (Gautier et al., 1993) or the Early Cretaceous trans-tensional basins now exposed within the Pyrenean mountain belt (e.g. Berástegui, et al., 1990). The influence of salt in its structuring is common for all of these examples.

Several complex fault systems of this kind are found in the Norwegian continental shelf such as the Hoop the Ringvassøy-Loppa and the Bjørnøya fault

complexes in the Barents Sea (e.g. Gabrielsen 1984; Gabrielsen et al. 1990; 1997; 2016 Faleide et al. 1993;), the Leirfallet and Bremstein fault complexes of mid Norway (Marsh et al. 2011; Wilson et al., 2013) and the Egersund area of the North Sea (e.g. Kane et al. 2010; Marsh et al. 2010; Jackson et al. 2013; Jackson & Lewis 2013; Tvedt et al. 2016) illustrate the need for a better understanding of relationships between graben configurations and fault geometries and their vertical linkage in sedimentary sequences of mechanical contrasts.

We apply physical analogue experiments, the effects of mechanically stratified systems (single and multiple décollement layers) on extensional geometries and fault connectivity upon single and polyphase deformation events. These novel experiments are complementary to previously published studies using single décollements in extensional systems (e.g. Withjack & Callaway, 2000, Brun & Choukroune, 1983, Bahroudi et al., 2003; Gabrielsen et al. 2016).

Set-up and conditions for the analogue experiments

The present experiments were performed at the Tectonic Laboratory (TecLab) at Utrecht University and consisted of stratified brittle-ductile systems with layered sequences of sieved sand (brittle layers) of similar composition and grain size, interlayered with silicone putty (SGM-36 Dow Coming; see Weijermars et al. 1993) representing ductile layers.

All experiments were built on a 1 mm thick plastic sheet (40x40 cm) that was placed on a flat, horizontal table surface (**Figure 1a**). The coloured layers of sieved quartz sand had a grain size of 300 μm, density of 1510 kgm^{-3}, cohesion of 30-70 Pa and a coefficient of friction of 0.6. The feldspar sand had a grain size of 300 μm, cohesion of c. 15 Pa, a density of 1300 kgm^{-3}. The feldspar sand grains were, more angular with an internal friction coefficient of 0.75 as an average (see also Sokoutis et al. 2005: Willingshofer et al. 2005; Luth et al., 2010). The layered models were scaled so that 10 mm in the model approximates 1 km in nature (for scaling calculations, see McClay 1990, Brun et al. 1994).

In all cases extension was applied by pulling a basal plastic sheet at a constant rate of 1 cm/hr. The contact between the fixed and movable base define a

velocity discontinuity, “VD” (Ballard J-F. et al. 1987; Tron V. and Brun J-P. 1991) . In all experiments, care was taken to prevent silicone layers coming into direct contact with the sidewalls in order to avoid unwanted border effects due to enhanced friction. The development of the structural configurations was documented by taking one top-view photograph for each centimeter of extension. When complete, the experiments were covered with a thin layer of sand to stabilize the structures and the surface topography. After deformation, the models were soaked in water and cut into longitudinal stripes to expose cross sections for photographs of the internal structures. In the experiments where two phases of extension were utilized, the second phase of extension was applied following the emplacement of a second layer of silicon polymer and filling of the earlier formed grabens with sand. This sequence accordingly represented a second cycle of sedimentation. Finally, the results of the experiments with one phase of extension were compared to results with two phases of co-axial extension. Emphasis was paid to the reactivation of faults in response to the second phase of extension.

In the present analysis, the series 1 experiments, consisting of a homogeneous quartz or quartz-feldspar sand sequence (**Figure 1b**) serves as a reference to the other experiments. Series 2 and 3 experiments were sand-silicone models in which one (series 2) or two (series 3) layers of silicone were embedded in the sand (**Figure 1c,d).** The series 2 experiments where one detachment layer was utilized, are relevant to the Halten Terrace and the North Sea, which are both characterized by one dominant salt layer of Triassic and Permian salt, respectively (Marsh et al. 2010, 2011; Wilson et al., 2013; Kane et al. 2010; Jackson et al. 2013). The series 3 experiments are of particular relevance to the Barents Sea area, because this series utilized two layers of mechanical contrast, which compares to the evaporate- and mudstone-sequences in that area (Mahajan et al. 2014; Gabrielsen et al. 2016).

The experiments with two phases of extension are of particular interest to e.g. the Hoop fault Complex of the Barents Sea, where two phases of extension are likely to have occurred (Mahajan et al. 2017; Gabrielsen et al. 2016).

Experimental Results

In the following we describe the general development and the final geometries of each experimental series, utilizing information from individual experiments to illustrate variations within each experimental series. Detailed information about the set-up and conditions for each model are given in **Table 1**.

Experiment Series 1:

Series 1 experiments, which utilize mechanically homogeneous sand sequences, produced an overall similar structural style. As a typical example, **Experiment S1-1** was performed by extending a 10 cm thick sequence of homogenous quartz sand by totally 9 cm in one stage. The initial stage of deformation resulted in a symmetrical graben, the axis of which was oriented orthogonally to the extension direction. The first faults became visible on the surface on both sides of the graben after 1 cm of extension (**Figure 2a**). Normal faults continued to develop on the in the footwall block by sequential footwall collapse (**Figure 2b-d**), so that the oldest faults were found in the inner part of the graben. On the side of the moving block, deformation was focused in one relatively stable fault zone that widened and accumulated the displacement as deformation proceeded, producing a more asymmetrical graben as the experiment proceeded (**Figure 2d**).

The asymmetric final configuration is evident in the final experiment S1-1 cross-sections (**Figure 3a,b**), which was characterized by an array of normal faults affecting the entire sequence, and dipping towards the graben axis on the fixed (proximal) side and an oppositely dipping distinct, 5 mm wide master fault zone defining the graben margin at the side of the moving (distal) block. Each fault was generally planar, but with a listric shape towards its base.

Experiment S1-2 (**Table 1**) differed from S1-1 in that it utilized quartz sand in the lower half of the experiment and feldspar sand in the upper half, creating a strength contrast within the total sequence (see information about sand types above). Furthermore, extension was performed in two stages. Thus, after 6 cm of extension, the experiment was stopped and a sequence of feldspar sand was

sieved on top of the experiment before the second stage of extension was started. By the end of the second stage (6 cm of extension), the total graben width (as observed at the surface) was less than that in Experiment S1-1, which is also obvious from the analyzed cross sections. The cross-section of the final stage display two vertically fault systems. The deepest of these is affiliated with the deepest part of the basin and developed in the first deformation stage. This fault system was wider than the system associated with the second stage of extension affecting the shallower feldspar sand layers.. There was no detachment between the two layers, so that the faults of the top layer continue without interruption into the lower layer showing that the inner parts of the two fault systems at the two levels of became hard-linked during the second phase of extension. In contrast, the marginal (distal) faults in the stationary wall of the experiments remained isolated and stable structure during the second stage.

Experiment Series 2

In experiment series 2, a layer of silicon polymer was introduced in the sequence (**Table 1**), and the experiments were performed with two separate stages of extension. Thus, the experiments were halted after the first stage of extension, and a silicone polymer layer and a sand sequence of equal thickness to that used in stage 1 was deposited on the surface (48 mm above the base of the experiment) from the first deformation stage after smoothing the relief by sieving sand on it. The three experiments of series 2 displayed almost identical development and final geometries (**Figure 4**). In the first stage of these experiments asymmetrical grabens with an array of synthetic faults facing the graben axis above the fixed fault block and a wide fault zone above the moving block were produced (**Figure 4**). This is similar to the geometry obtained in experiment S1-1 and the first stage of experiment S1-2 (see above), as expected, because the experimental set-up and conditions were identical for these parts of the experiments.

After depositing the silicone polymer layer and the upper sand, sequential extension was restarted. In all series 2 experiments an elongated sag-area started to develop orthogonally to the direction of stretching and above the

buried graben axis (velocity discontinuity) from the first deformation stage, after c. 12.5% of total extension. As seen on the surface display, the second stage of the series 2 experiment was characterized by a much wider, asymmetric horst-and-graben system with an asymmetric central halfgraben situated above a wide, broken (**Figure 4a**) or intact (**Figure 4b**) a fault block that rotated towards the graben axis, defining a half graben. The large fault blocks were delineated by anti-listric, normal faults that were rotating towards the graben axis during transportation towards the graben center of the fault block itself (**Figure 4**), lkely due to sliding of the fault block on the silicon polymer layer. All faults in this stage in series 2 were rooted in the silicon polymer layer**,** and were generally not linked with the faults of stage 1. The only exception from this was the border faults that were soft-kinked to the deeper faults in all series 2 experiments. All faults in the upper fault system were planar, except for those in the middle graben that were upward steepening.

Experiment Series 3

In this series of experiments, a second ductile layer with similar mechanical properties and dimensions to that used in series 2 was included so that the two silicon layers were situated 30 and 66 mm above the base of the modeI (**Figure 1; Table I).** In Experiment S3-1 the model was extended in one stage (totally 4 cm of the total length of the experiment), whereas two phases of extension (2 + 2 cm) were adopted for experiments S3-2 and S3-3, with the upper silicone layer being placed after the first phase of extension.

All experiments produced an axial sag structure after 6% of extension. This structure was bordered by two separate narrow, distinct grabens. The first faults appeared at the surface on the side of the stable block of the sag area after 10% of extension, whereas the earliest faults on the opposite side of the sag area appeared slightly later. Thereafter, two more distinct grabens became visible at the surface on both flanks of the primary graben. All graben units subsided in concert until the termination of extension.

The final profiles show that the first-stage structures in experiments S3-1 and S3-2 portray simple, slightly asymmetrical grabens that were characterized by a contrasting number of faults at the two flanks and with rotated graben flanks related to sliding on the lowermost ductile layer. The central part of these grabens was situated right above the basal discontinuity (VD). This is identical to what was observed in the series 1 and the first stage of the series 2 experiments.
The second stage of extension produced similar, but wider structures in the two upper sand layers, as compared to the ones of the deepest sand layer. The faults displayed both hard-linked and soft-linked relations between the levels 1 and 2 and between levels 2 and 3, respectively (**Figure 5**). The hard-linked faults mainly occurred in the boundary faults of the graben.
The experiments of series 3 were stopped by a total extension of 4 cm, because the lowermost sequence was thinned to less that 1 cm.

In conclusion; by adding the second ductile layer and the upper sequence of sand, e.g. experiment S3-2, three distinct, separate strata-bound fault systems formed (**Figure 5)**. The graben structures widened stepwise from the bottom to the top sand sequences. As in the experiments of the two previous series, the deepest fault system generated an asymmetric graben. In contrast, the middle and upper sand units were delineated by symmetric grabens. The faults were generally planar. Exceptions are upward-steepening faults, which were related to the rotation of the marginal fault blocks.

Discussion and reflection seismic examples

The present series of experiments demonstrates the influence of multiple décollement horizons on the basin (graben) formation as well as on fault styles and fault linking mechanisms in stacked sediment sequences with variable mechanical strength. They also show that the complexity of the graben geometries are sensitive to even minute such contrasts (e.g. quartz and feldspar sand) and that the complexity increases for systems with multiple décollement

horizons and polyphase deformation. This is similar to that reported for contractional systems by e.g. Soleimany et al. (2013) and Santolaria et al. (2015).

Thus, the experiments performed with a mechanically homogeneous sequence (experiment 1-1 - quartz sand) and one stage of extension, displayed a graben asymmetry in that an array of sub-parallel extensional planar faults with listric lowermost parts developed in the stationary fault block, whereas the displaced block rather developed a zone with one dominant fault that remains stable with increasing strain (**Figure 6a**). This geometry was probably ruled by the displacement of the basal velocity contrast In contrast, the stratified experiment 1-2 (quartz- and feldspar sand) resulted in an up-section narrowing of the graben width in the feldspar sand sequence at the top of the experiment. This is likely due to the enhanced strength (greater friction) in the feldspar sand and means that up-section-narrowing graben systems can be expected in sedimentary sequences of inverted mechanical strength, and that a downward narrowing is the normal situation due to compaction and increasing mechanical strength with depth.

When one silicon putty layer was introduced between the quartz sand sequences, two distinct intra-formational soft-linked or unlinked fault systems (below and above the silicone polymer layer) formed. In these experiments, the fault system associated with the deeper sand layer was similar to that developed of experiment series 1 (sand sequences without silicon putty layer). The fault system affiliated with the second extension stage (above the décollement layer) displayed a strikingly different development and geometry; The deformation activated a wider panel than that seen for the faults below the décollement (stage1) and included some upward-steepening and rotated faults producing apparent reverse faults with anti-listric geometries The reason for this contrast in geometry was likely that the faults of the upper sequence were associated with basinward tilted fault blocks that had been trapped at the margins of the first-stage graben structures, where the silicon polymer layer had been substantially thinned, and were subject to gravitational gliding directed towards (the deepening) graben axis (**Figure 4**). Such unstable/sliding fault blocks on

311 basin margins are known from several places at the mid Norwegian continental
312 shelf; e.g. the Mikkel structure (Withjack & Callaway (2000) and Revfallet Fault
313 Complex (Dooley et al. 2003). Extensional faults with apparent reverse
314 geometries are promoted by strong contrasts in mechanical stiffness where the
315 stronger layer is the deepest (Horsfield 1977, Withjack et al. 2002). Hence, the
316 fault pattern of the upper sand sequence was completely at stake with that of the
317 lowermost sand unit. Although not very common, such geometries are found in
318 several places in the vicinity of basins with active syn-faulting halokinesis
319 (Harvey & Stewart 1998) One example from the Vingleia Fault Complex of Mid
320 Norway is shown in **Figure 6b**.
321
322 By adding a second ductile layer a third strata bound fault population developed
323 in the uppermost brittle unit. The faults and the master faults at the uppermost
324 level had either hard-linked, soft-linked or non-linked relations to faults at
325 deeper levels (**Figure 5**), allowing for differential strain to be accumulated for
326 each layer. The faults in each sand unit seemed to be nucleated at the lower
327 contact between the silicon putty and the sand, in some cases generating blind
328 faults. Contrasts in fault frequency and style when comparing the deep and
329 shallow sand sequences separated by silicon putty as observed in the
330 experiments of Series 2 and 3 is similar to observations reported for natural fault
331 systems by for the Channel Basin of southern England (Harvey & Stewart 1998),
332 for the for the Bremstein and Revfallet fault complexes offshore mid Norway
333 (Dooley et al. 2003; Wilson et al. 2013), for the Sembo relay system offshore
334 Angola (Dutton & Trudgill 2009) and for several fault systems elsewhere
335 (Withjack & Callaway 2000). The effects of mechanically stratified sequences on
336 fault populations at different stratigraphic levels are, therefore, well established
337 in nature.
338 By further extension it is likely that the master fault systems in these arrays
339 would become hard-linked in the vertical dimension, generating a consistent
340 system of faults like that reported by Harvey & Stewart (1998), Jackson & Lewis
341 (2012), Jackson et al. (2013) and Gabrielsen et al. (2016). In experiment series 2
342 and 3 fault vertical fault linkage was promoted where layers of silicone polymer
343 remained intact. Accumulated heave associated with repeated reactivation as

reported from the Barents Sea by Mahajan et al. (2014). This observation is also consistent with analogue experimental results obtained by Withjack & Callaway (2000) and Withjack et al (2002) and Dooley et al. (2003) (**Figure 6c**), In the cases where the silicon polymer became unevenly thinned and even thinned to zero, vertically stacked regimes of contrasting geometry and the rotation of fault blocks towards the basin center was common, the fault block riders sometimes becoming stuck at the graben margins where the silicon polymer was thinned the most (**Figure 6b**). In summary, the experiments shed light on the mechanisms leading to composite and complex fault geometries sometimes observed in reflection seismic data.

Conclusions

The three series of experiments demonstrated that:

(1) the deepest fault system developed in homogeneous quartz sand produced a very robust and asymmetric graben geometry with deformation being localized along a wide and diffuse fault at the moving (distal with respect to the stationary fault block) flank of the graben whereas strain was distributed over several discrete faults at the stationary proximal) flank. This development was similar in all one-stage and first-stage on layer experiments.

(2) In experiments with one or several weak layers (silicon polymer) fault systems of the middle and upper sand units (above silicon putty layers) had significantly different configurations from the fault systems in the layers below the silicon putty. For the three-layer (sand-silicon-sand) system configurations were dramatically different for the two sand sequences. In these experiments large, rotated fault blocks delineated by anti-listric faults with a reverse throw developed above the graben margin master faults. These were affected by gravitationally induced sliding of the fault blocks across the deeper graben margins. The fault systems in deep and shallow sequences were generally un-linked. It is inferred that this pattern is strongly influenced by the gravitational forces due to basin-ward sliding of the uppermost fault block

(3) The three-layer systems produced relatively symmetrical upward-widening graben structures with a stronger tendency for soft-linking and hard-linking between the deep and shallow faults, generating more stable, but upward widening graben structures. The gravitational component causing basinward fault block sliding was less pronounced in these experiments.

(4) We find that some of the depth-dependent and composite graben geometries as well as complex fault geometries developed in the present experiments explains some less well explained geometries in extensional structures observed in the Norwegian continental shelf.

Acknowledgements

Background for the experiments were based on seismic intrepretations by Agus Fitriyanto and Aatisha Mahajan. An early version of the manuscript benefited much from careful review, thoughtful comments and discussion with C.A.L. Jackson at …. and ananonymous colleague

The study is a part of the ArcEx-project and was supported by the Norwegian Research Council (228107/E30) and industry partners.

Figure captions

Figure 1 a) Horizontal view of the experimental setup. b) Schematic section showing construction of Experiment series 1 (only basal silicon polymer layer). c) Schematic section showing the construction of experiment series 2 (One level of silicon polymer). d) Experimental set-up for experiment series 3. Redrafted from Gabrielsen et al. (2016).

Figure 2a-d; Top-view photographs showing the step-wise development of experiment S1-1 after 1, 3, 5 and 7 cm of extension. Arrow indicates direction of the moving block.

Figure 3: Top views and cross sections of Experiments S1-1 and S1-2 of experiment series 1 after fulfilled extension (9cm; 22.5%). a) Experiment S1-1 was performed with only quartz sand and one stage of extension. Note different fault styles for the two-graben margins. b) Experiment S1-2 was performed with

quartz sand in the first stage (base; gray) and feldspar sand (top; white) in the second stage. Note the wider area of faulting associated with the first stage compared to the narrower graben associated with the second stage of extension. See text for full description.

Figure 4: Map view and cross-sections for experiments three experiments (1-3) of experiment series 2. These experiments were performed with one layer of silicon putty separating a lower and an upper sand sequence. Both sequences were quartz sand. Note contrast in graben geometry between stages 1 and 2, and the complex system of lined grabens and the large, basinward-rotated fault block that was common for stage 2 for all experiments. See text for full description.

Figure 5: Map view of and cross-sections of S3-1 and S3-2 of experiments of series 3 (two layers of silicon polymer separating three sequences of quartz sand). Note the generally symmetrical grabens at all levels and the upward increasing graben width. See text for full description.

Figure 6: Comparison between experiments and observed fault/graben geometries at the Norwegian continental shelf. a-b) graben with contrasting fault geometry at the two margins. Experiment S1-1 and the margin of the Fingerdjupet Subbasin, southwestern Barents Sea. c-d) Upward-steepening anti-listric fault at graben margin with sliding fault block. Experiment S2-2 and seismic example from the Vingleia Fault Complex, mid Norway. e-f) graben systems developed above weak layers where graben marginal fault steps towards the footwall for each structural level, resulting in stepwise increasing the up-section graben width. Experiment S3-6 and seismic example from the Hoop Fault Complex, southwestern Barents Sea.

Table 1: Summary of set-up and conditions for experiment used in the present analysis. The experiments were divided into three series: Series 1 consisted of sand only. Series 2 and 3 utilized one and two layers of silicon polymer respectively. The experiments were performed with single and polyphase extension and different bulk extension (columns 7 and 8).

464
465
466 **References**
467
468 Anell,I., Braathen,A., Olaussen,S. & Osmundsen,P.T., 2013: Evidence of faulting
469 contradicts a quiscent northern Barents Shelf during the Triassic, First Break, 31, 67-
470 76.
471
472 Bahroudi, A., Koyi, H. A., & Talbot, C. J., 2003: Effect of ductile and frictional
473 décollements on style of extension. Journal of Structural Geology, 25(9), 1401-1423.
474
475 Ballard J-F ., Brun J-P. et Van Ven Driessche J.,1987: Propagation des
476 chevauchements au-dessus des zones de décollement: modèles expérimentaux.
477 Comptes Rendus de l'Académie des Sciences, Paris, 11, 305, 1249-1253.
478
479 Berástegui, X., J. García-Senz, and M. Losantos (1990), Tecto-sedimentary evolution
480 of the Organyà extensional basin (central south Pyrenean unit, Spain) during the
481 Lower Cretaceous, Bull. Soc. Geol. Fr., 8(VI 2), 251–264,
482 doi:10.2113/gssgfbull.VI.2.251.
483
484 Briggs, S. E., Davies, R. J., Cartwright, J. A., & Morgan, R. (2006). Multiple
485 detachment levels and their control on fold styles in the compressional domain of the
486 deepwater west Niger Delta. Basin Research, 18(4), 435-450.
487
488 Brun, J. P., & Choukroune, P.,1983: Normal faulting, block tilting, and decollement
489 in a stretched crust. Tectonics, 2(4), 345-356.
490
491 Brun,J.-P., Sokoutis,D., & van den Driessche,J., 1994: Analogue modelling of
492 detachment fault systems and core complexes, Geology, 22, 319-322.
493
494 Bruton, D. L., Gabrielsen, R. H. & Larsen, B. T, 2010.: The Caledonides of the Oslo
495 Region, Norway- stratigraphy and structural elements. Norwegian Journal of
496 Geology, 90, 93-121.
497
498 Chapman,J.B. & McCarty,R.S., 2013: Detachnent levels in the Marathon fold and
499 thrust belt, west Texas, Journal of Structural Geology, 49, 23-34,
500 doi:10.1016/j.jsg.2013.01.007.
501
502 Dooley, T., McClay, K. R., & Pascoe, R. 2003: 3D analogue models of variable
503 displacement extensional faults: applications to the Revfallet Fault system, offshore
504 mid-Norway. Geological Society, London, Special Publication, 212, 151-167.
505
506 Dutton,D.M. & Trugill,B.D., 2009: Four-dimensioal analysis of the Semdo relay
507 system, offshore Angola: Implications for fault growth in salt-detached settings,
508 American Association of Petroleum Geologists Bulletin, 93, 763-794.
509
510 Edwards,M.B., 1976: Growth faults in Upper Triassic deltaic sediments, Svalbard.
511 American Association of Petroleum Geologists Bulletin, 60(3), 341-255.
512
513 Faleide,J.I., Vågnes,E. & Gudlaugsson,S.T.,1993: Late Mesozoic - Cenozoic

514 evolution of the south-western Barents Sea in a regional rift-shear tectonic setting.
515 Marine and Petroelum Geology, 10, 186-214.
516
517 Fossen,H. & Gabrielsen,R.H., 1995: Experimental modeling of extensional fault
518 systems by use of plaster. Journal of Structural Geology, 18(5), 673-687.
519
520 Froitzheim, N., & Eberli, G. P. (1990). Extensional detachment faulting in the
521 evolution of a Tethys passive continental margin, Eastern Alps, Switzerland.
522 Geological Society of America Bulletin, 102(9), 1297-1308.
523
524 Gabrielsen, R.H., 1984: Long-lived fault zones and their influence on the
525 development of the southwestern Barents Sea. Journal of the geological Society of
526 London, 141(4), 651 - 662.
527
528 Gabrielsen,R.H., Færseth,R.B., Jensen,L.N., Kalheim,J.E. & Riis,F.,1990: Structural
529 elements of the Norwegian Continental Shelf. Part I: The Barents Sea Region.
530 Norwegian Petroleum Directorate, Bulletin, 6, 33pp.
531
532 Gabrielsen,R.H., Grunnaleite,I. & Rasmussen,E., 1997: Cretaceous and Tertiary
533 inversion in the Bjørnøyrenna Fault Complex, south-western Barents Sea. Marine and
534 Petroleum Geology, 14(2), 165-178.
535
536 Gabrielsen,R.H., Sokoutis,,D., Willingshofer,E. & Faleide,J.I., 2016: Fault linkage
537 across weak layers during extension: An experimental approach and consequence in
538 the Hoop Fault Complex of the southeastern Barents Sea, Petroleum Geoscience,
539 22(2), 123-135.
540
541 García-Dueñas, V., Balanyá, J. C., & Martínez-Martínez, J. M. (1992). Miocene
542 extensional detachments in the outcropping basement of the Northern Alboran Basin
543 (Betics) and their tectonic implications. Geo-Marine Letters, 12(2-3), 88-95.
544
545 Gautier, P., Brun, J. P., & Jolivet, L., 19993: Structure and kinematics of upper
546 Cenozoic extensional detachment on Naxos and Paros (Cyclades Islands, Greece).
547 Tectonics, 12(5), 1180-1194.
548
549 Gibbs, A.D.,1984): Structural evolution of extensional basin margins. Journal of the
550 Geological Society, 141(4), 609-620.
551
552 Grelaud, S., Vergés, J., Nalpas, T., & Karpuz, R. (2003, April). Impact of multiple
553 detachment levels on deformation of external fold-and-thrust belts. in: EGS-AGU-
554 EUG Joint Assembly, 1, p. 11003.
555 Harvey, M. J., & Stewart, S. A. (1998). Influence of salt on the structural evolution of
556 the Channel Basin. Geological Society, London, Special Publications, 133(1), 241-
557 266.
558
559 Horsfield,W.T., 1977: An experimental approach to basement-controlled faulting.
560 Geologie en Mijbouw, 56(4), 3634-370.
561

562 Jackson,C.A.L., Chua,S.T., Bell,R.E. & Magee,C., 2013: Structural style and early
563 stage growth of inversion structures: 3D seismic insights from the Egersund Basin,
564 offshore Norway, Journal of Structural Geology, 46, 167-185.
565
566 Jackson,C.A.L.,& Lewis,M.M., 2012: Origin of an anhydrite sheathencircling a salt
567 diapir and implications for the seismic imaging of steep-sided salt structures,
568 Egersund Basin, Northern North Sea. Journal Geological Society, 169(5), 593-599,
569 doi:10.1144/0016-76482011-126.
570
571 Jackson,C.A.L. & Lewis.,M.M., 2013: Physiography of the NE margin of the Permian
572 Salt Basin: hew insights from 3D seismic reflection data, Journal Geological Society
573 London, 170(6), doi: 10.1144/jgs2013-026.
574
575 Jackson,C.A.-L. & Lewis,M.M., 2016: Structural style and evolution of a salt-
576 infuenced basin margin: impact of variations in salt composition and the role of
577 polyphase extension, Basin Research, 28(1), 81-102, doi: 10.1111/bre 12099.
578
579 Kane,K.E., Jackson,C-A.L. & Larsen,E., 2010: Normal fault growth and fault-related
580 folding in a salt-influenced rift basin: south Viking Graben, offshore Norway, Journal
581 of Structural Geology, 32, 490-506.
582
583 Koyi, H., & Petersen, K.,1993. Influence of basement faults on the development of
584 salt structures in the Danish Basin. Marine and Petroleum Geology, 10(2), 82-94.
585
586 Latta, D.K. & Anastasio, D.J., 2007): Multiple scales of mechanical stratification and
587 décollement fold kinematics, Sierra Madre Oriental foreland, northeast
588 Mexico. Journal of Structural Geology, 29(7), 1241-1255.
589
590 Mahajan,A., Gabrielsen,R.H. & Faleide,J.I., 2014: Structural analysis of 3D seismic
591 for the Hoop Fault Complex, SW Barents Sea (abstract), in: S.Eriksen, H.Haflidason,
592 O.Olesen, H. Schiellerup & A.M.Husås (eds.): The Arctic Days Conference 2014,
593 Abstracts and Proceedings of the Geological Society of Norway, 2 -2014, 58.
594
595 Marsh, N., Imber, J., Holdsworth, R. E., Brockbank, P., & Ringrose, P.,2010: The
596 structural evolution of the Halten Terrace, offshore Mid- Norway: extensional fault
597 growth and strain localization in a multi- layer brittle–ductile system. Basin
598 Research, 22(2), 195-214.
599
600 McClay.K.R., 1990:Extensional fault systems in sedimentary basins. A review of
601 analogue model studies, Marine and Petroleum Geology, 7, 206-233.
602
603 Perrin.C., Clemenzi,L., Malaveille,J., Molli,G., Taboda,A. & Dominguez,S., 2013:
604 Impact of erosion and décollements on large-scale faulting and folding in orogenic
605 wedges: analogue models and case studies. Journal Geological Society London,
606 170(6), 893-904, doi: 10.1144/jgs2013-012.
607
608 Santolaria P., Vendeville B.C., Graveleau F., Soto R., Casas-Sainz A., 2015: Double
609 evaporitic décollements: Influence of pinch-out overlapping in experimental thrust wedges.
610 Journal of Structural Geology, 76, 35-51.
611

612 Sokoutis,D., Burg,J-P-., Bonini.M., Corti,G. & Cloetingh,S., 2005: Lithospheric-scale
613 structures from the perspective of analogue continental collision, Tectonophysics,
614 406, 1-15

615 Soleimany,T. Nalpas,T & Sàbat,F., 2013 Multidetachment analogue models of fold in
616 transpression: The NW Persian Gulf, Geologica Acta, 11 (3), 265 - 276, doi: 10 .1344 /105.
617 000001870

618 Stewart, I. J., 1993: Structural controls on the Late Jurassic age shelf system, Ula
619 trend, Norwegian North Sea. In Geological Society, London, Petroleum Geology
620 Conference Series, Geological Society of London, 4, 469-483.

621 Tron, V. & Brun J-P.,1991: Experiments on oblique rifting in brittle-ductile systems.
622 Tectonophysics, 188(1/2), 71-84.

623 Tvedt,A.B.M., Rotevatn,A. & Jackson,C.A.-L., 2016: Supra-salt normal fault growth
624 during the rise and fall of a diapir: Perspectives from 3D seismic reflection data,
625 Norwegian North Sea, Journal of Structural Geology, 91, 1-26, doi:
626 10.1016/jsg2016.08.001
627
628 Weijermars,R., Jackson,M.P.A. & Vendeville. B., 1993: Rheological and tectonic
629 modelling of salt provinces, Tectonophysics, 217, 627-651.
630
631 Wijns, C., Weinberg, R., Gessner, K., & Moresi, L. (2005). Mode of crustal extension
632 determined by rheological layering. Earth and Planetary Science Letters, 236(1), 120-
633 134.
634
635 Willingshofer,E., Sokoutis,D. & Burg,J.-P., 2005: Lithosprer-scale analogue
636 modelling of collsion zones with a pre-existing weak zone, *in*: Gapais,D.,
637 Brun.,J.P.& Cobbold,P.R. (eds.): DeformatiomMechanisms, Rhology and Tectonics:
638 from Minerals to the Litohsphere, Geological Society London Special Publication,43,
639 277-294.
640
641 Wilson, P ; Elliott, GM ; Gawthorpe, RL ; Jackson, CAL ; Michelsen, L ; Sharp, IR,
642 2013: Geometry and segmentation of an evaporate-detached normal fault array: 3D
643 seismic analysis of the southern Bremstein Fault Complex, offshore mid-Norway,
644 Journal Of Structural Geology, 51, 74-91.
645
646 Withjack, M. O., & Callaway, S.,2000: Active normal faulting beneath a salt layer: an
647 experimental study of deformation patterns in the cover sequence. American
648 Aasociation of Petroleum Geologists, Bulletin, 84(5), 627-651.
649
650
651
652

Figure

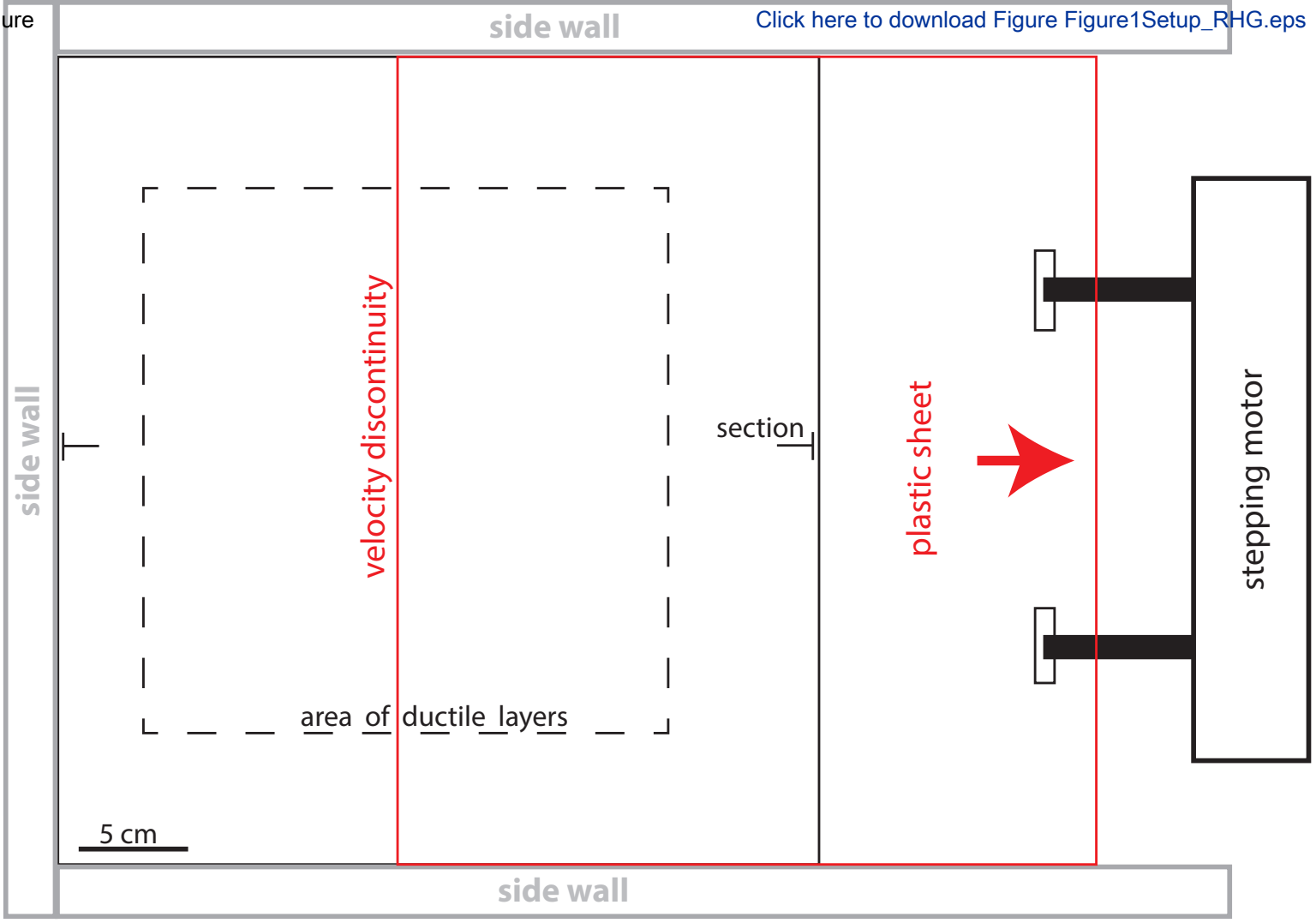

(a)

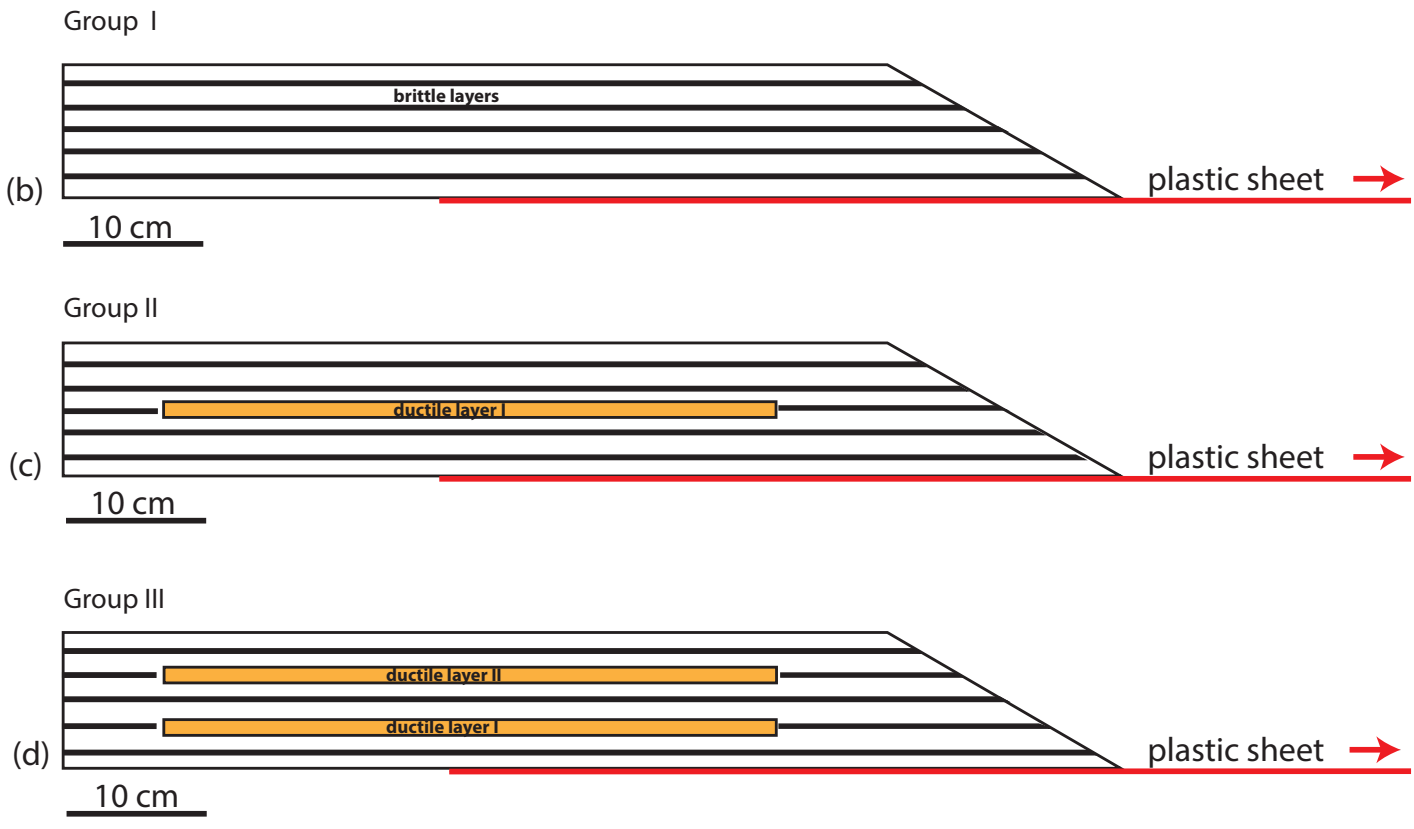

(b)

(c)

(d)

Figure 1

Figure

Click here to download Figure Figure2TopView_RHG_new.tif

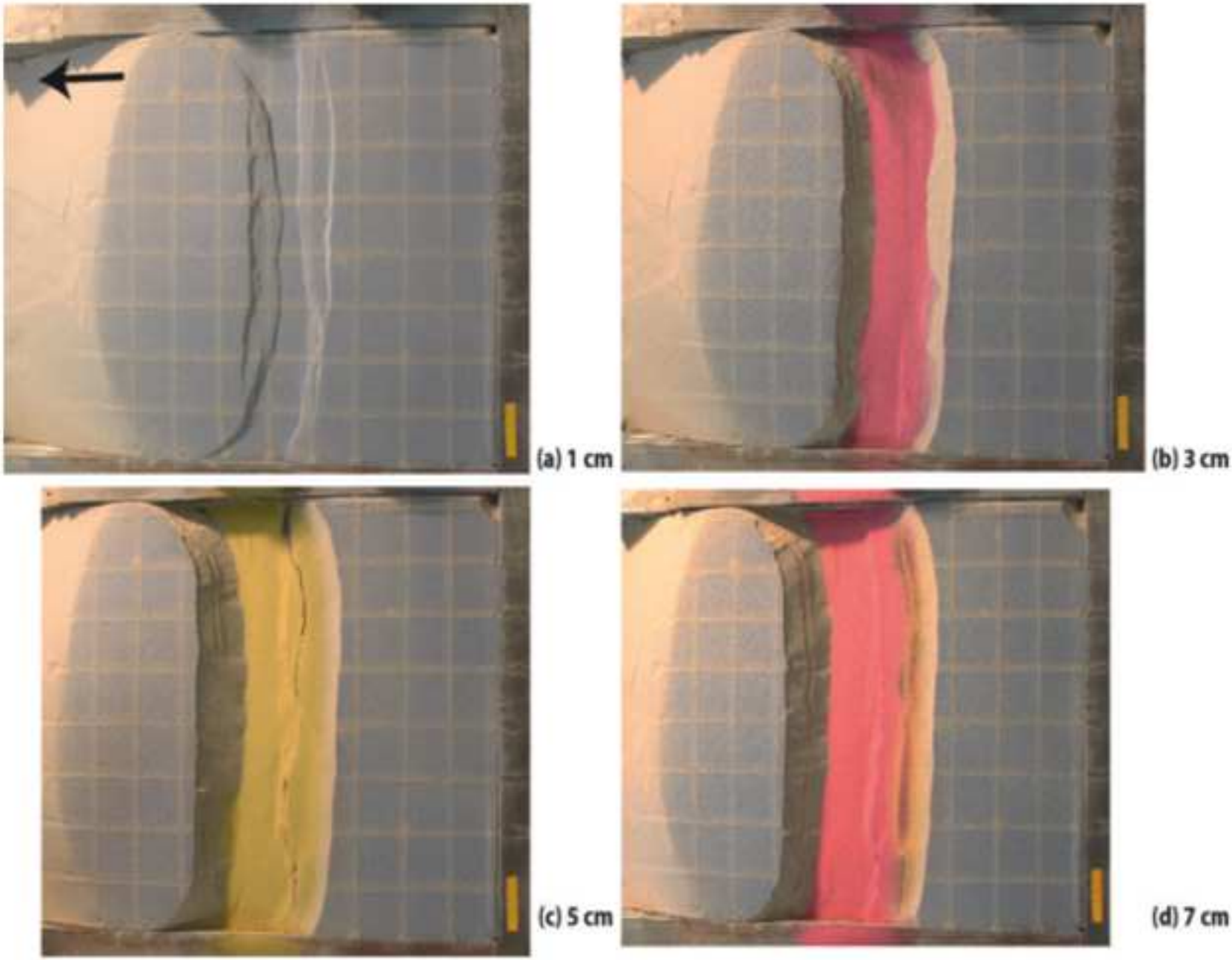

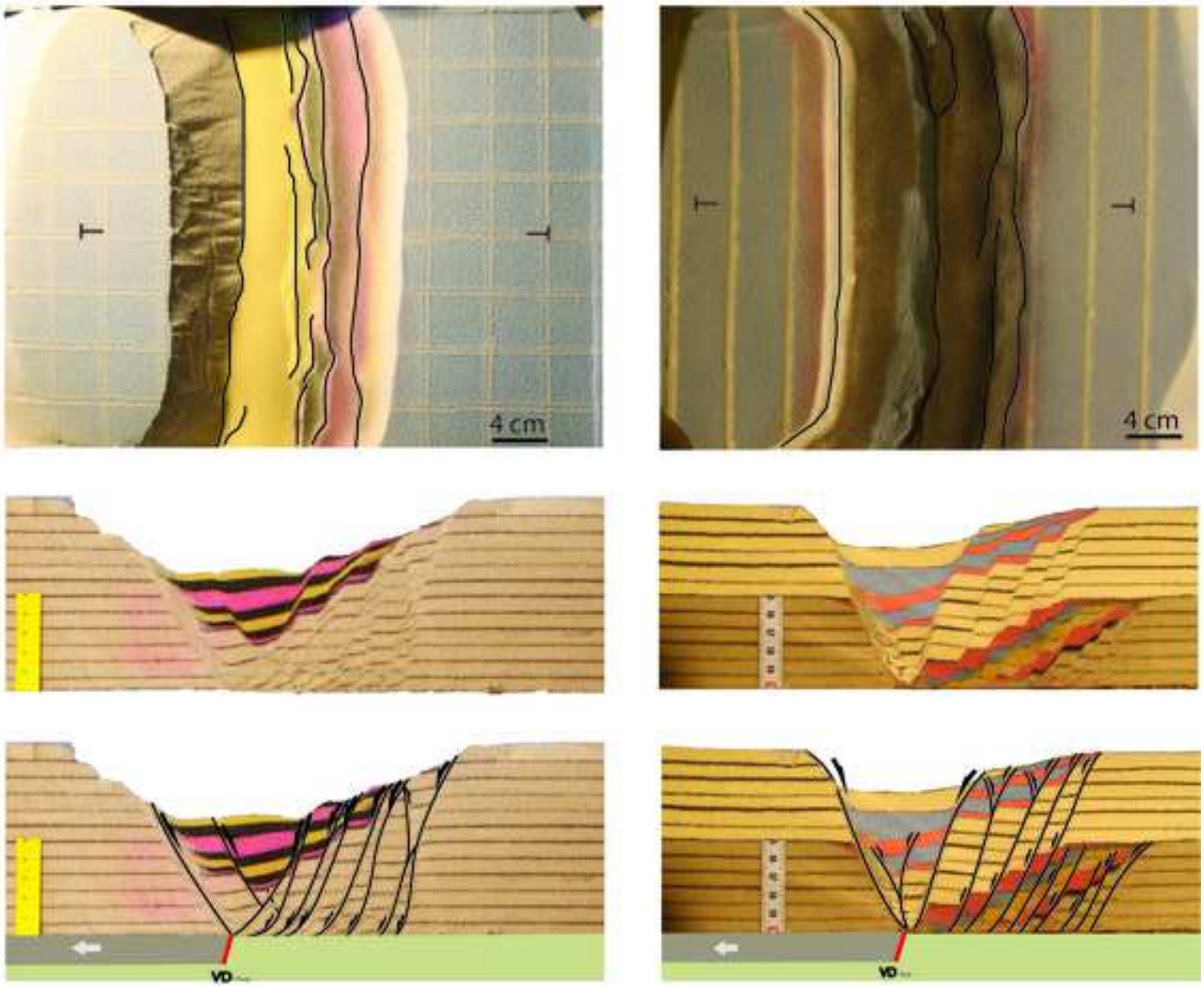

(a) (b)

Fig. 3

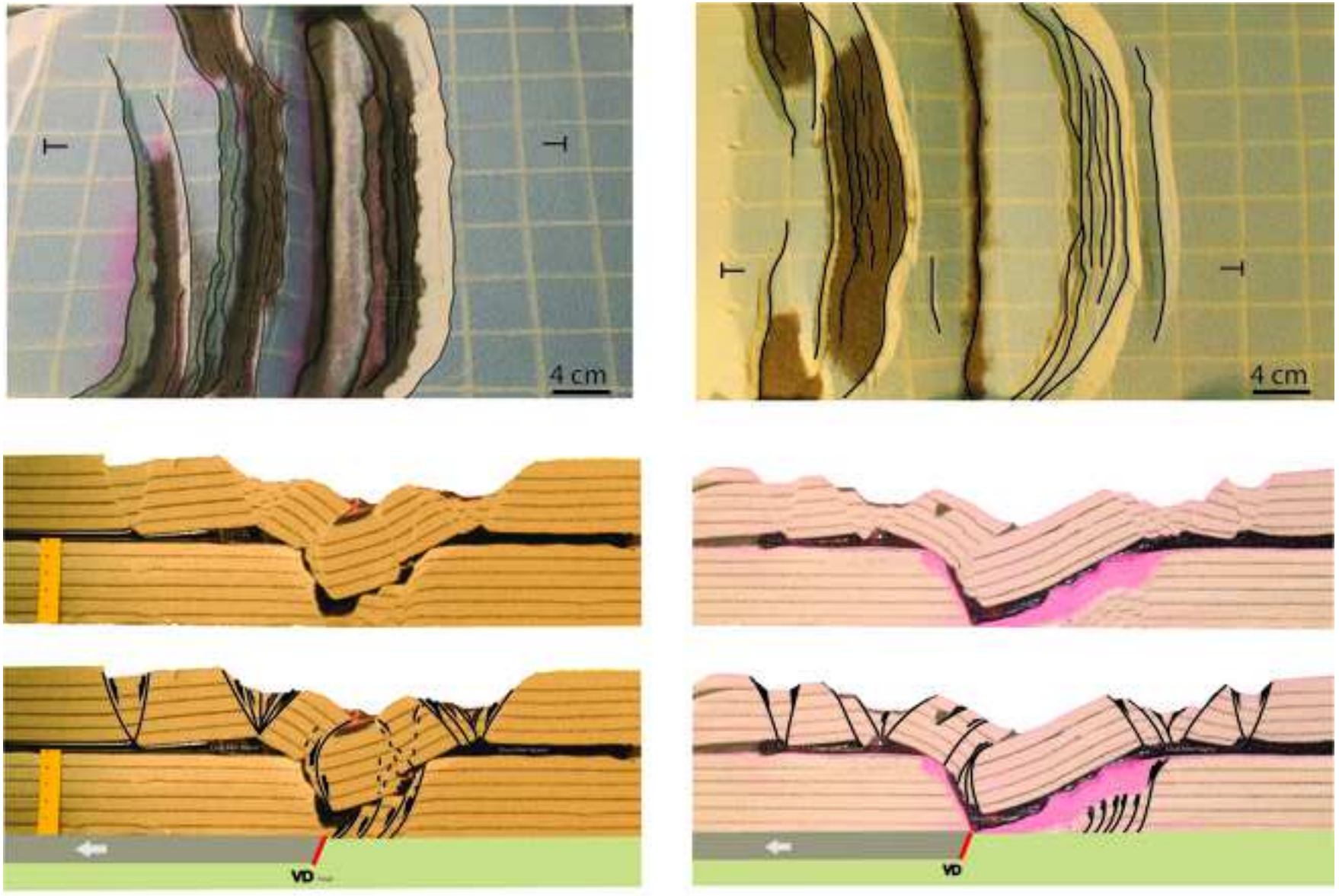

Fig. 4

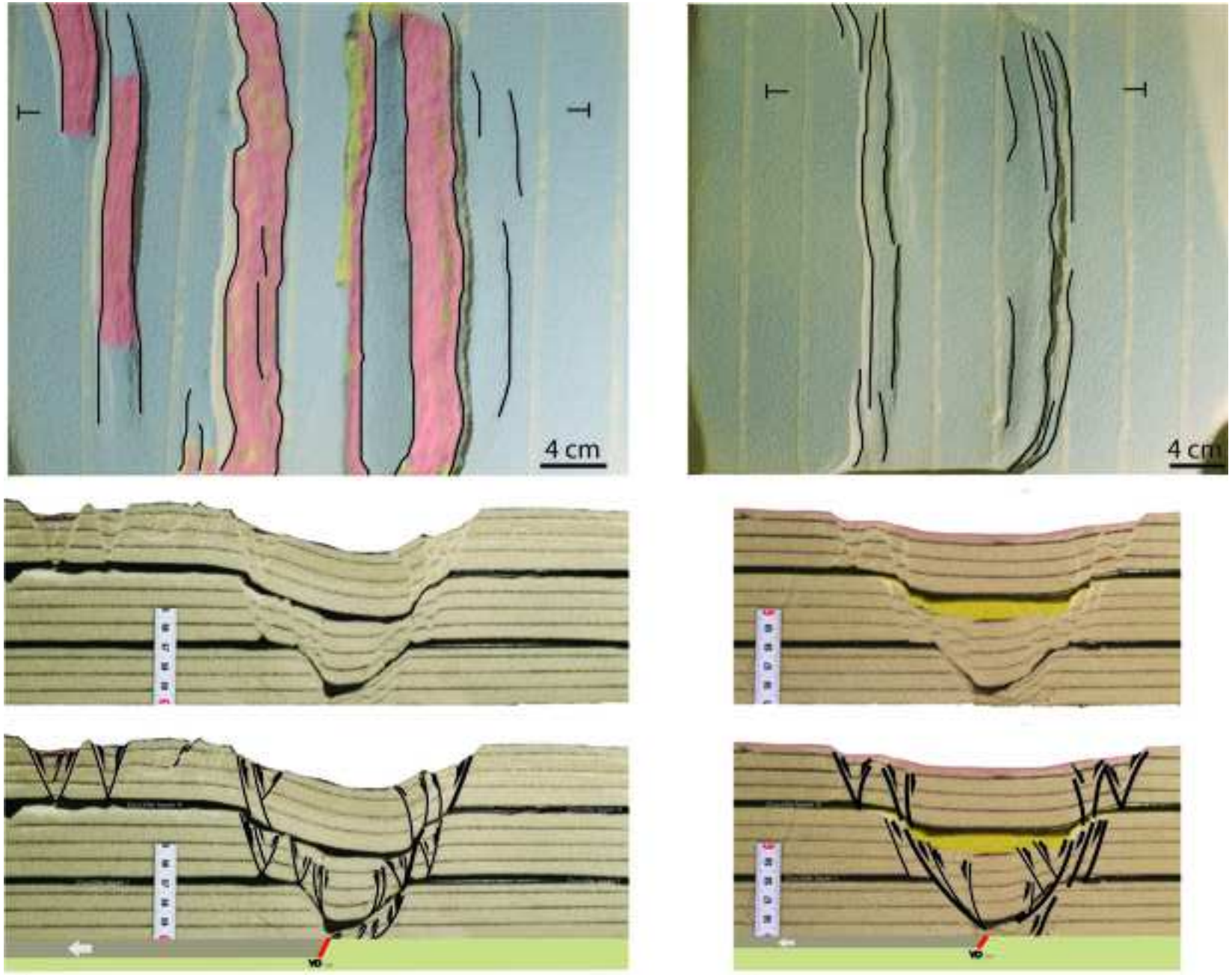

Fig. 5

Figure

Click here to download Figure Figure6ModSeis_RHG.tif

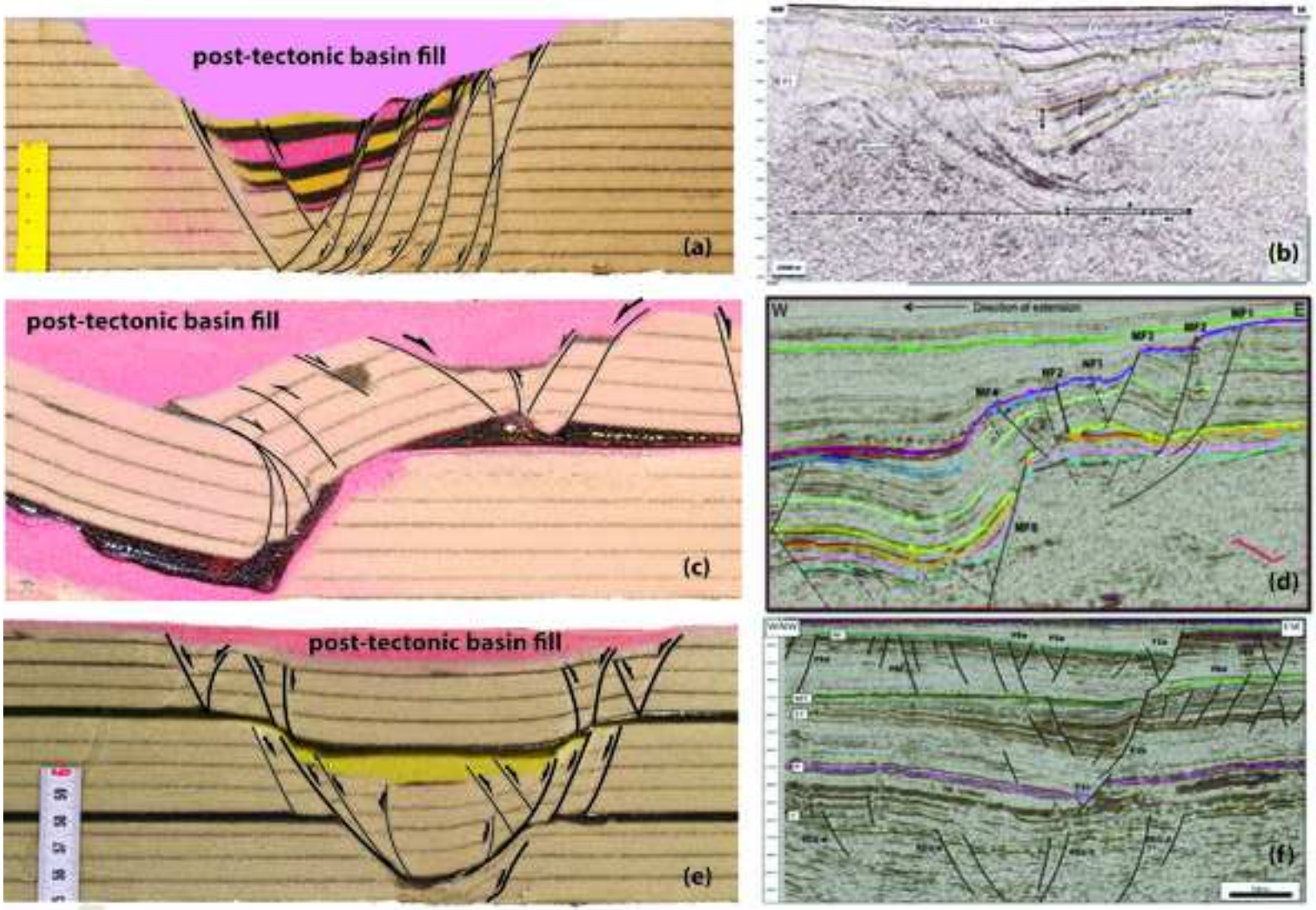

Fig. 6

Table 1

Experiment series	Expr.no	Materials	Sequence thickness (cm)	Silicone polym. layer thickness (cm)	Depth of s.p. Layer	Phases of extension	Total extension (cm)
1	1	Qtz sand	9.6	none		1	9
	4	Qtz sand fsp sand	10.0	none		2	6 + 6
2	2	Qtz sand one sp-layer	10.4	0.8	4.8	1	5
	3	Qtz sand one sp-layer	10.4	0.8	4.8	2	4 + 3
	8	Qtz sand one sp-layer glass beads	10.0	0.4	6.6	2	2 + 2
3	5	Qtz sand two sp-layers	9.8	0.4	3.0 and .,6	1	4
	6	Qtz sand two sp-layers	9.8	0.4	3.0 and .,6	2	2 + 2
	7	Qtz sand two sp-layers	9.8	0.4	3.0 and 6.6	2	2 + 2